# Multipath Removal by Online Blind Deconvolution in Through-the-Wall-Imaging

Mansour, H.; Kamilov, U.

TR2016-006 March 2016

**Abstract**

In this paper, we propose an online radar imaging scheme that recovers a sparse scene and removes the multipath ringing induced by the front wall in a Through-the-Wall-Imaging (TWI) system without prior knowledge of the wall parameters. Our approach uses online measurements obtained from individual transmitter-receiver pairs to incrementally build the primary response of targets behind the front wall and find a corresponding delay convolution operator that generates the multi-path reflections available in the received signal. In order to perform online sparse imaging while removing wall clutter reflections, we developed a deconvolution extension of the Sparse Randomized Kaczmarz (SRK) algorithm that finds sparse solutions to under- and over-determined linear systems of equations. Our scheme allows for imaging with nonuniformly spaced antennas by building an explicit delay-and-sum imaging operator for each new measurement. Moreover, the active memory requirements remain small even for large scale MIMO systems since the imaging operators are only constructed for individual transmitter-receiver pairs. We test our approach on a simple FDTD simulated room with internal targets and demonstrate that our method successfully eliminates multipath reflections while correctly locating the targets.

*2016 IEEE International Conference on Acoustics, Speech, and Signal Processing (ICASSP)*

# MULTIPATH REMOVAL BY ONLINE BLIND DECONVOLUTION IN THROUGH-THE-WALL-IMAGING

*Hassan Mansour, Ulugbek S. Kamilov*

Mitsubishi Electric Research Laboratories
Cambridge, MA 02139
Email: {mansour, kamilov}@merl.com

**ABSTRACT**

In this paper, we propose an online radar imaging scheme that recovers a sparse scene and removes the multipath ringing induced by the front wall in a Through-the-Wall-Imaging (TWI) system without prior knowledge of the wall parameters. Our approach uses online measurements obtained from individual transmitter-receiver pairs to incrementally build the primary response of targets behind the front wall and find a corresponding delay convolution operator that generates the multi-path reflections available in the received signal. In order to perform online sparse imaging while removing wall clutter reflections, we developed a deconvolution extension of the Sparse Randomized Kaczmarz (SRK) algorithm that finds sparse solutions to under- and over-determined linear systems of equations. Our scheme allows for imaging with nonuniformly spaced antennas by building an explicit delay-and-sum imaging operator for each new measurement. Moreover, the active memory requirements remain small even for large scale MIMO systems since the imaging operators are only constructed for individual transmitter-receiver pairs. We test our approach on a simple FDTD simulated room with internal targets and demonstrate that our method successfully eliminates multipath reflections while correctly locating the targets.

***Index Terms***— Through-the-wall-imaging, multi-path elimination, sparse recovery, blind deconvolution, Kaczmarz iterations

## 1. INTRODUCTION

Through-the-wall-imaging (TWI) is a promising and widely investigated technique for detecting objects inside enclosed structures [1]. In a typical scenario, a source emits an electromagnetic (EM) radar pulse which propagates through the outside wall of the structure, reflects off the internal targets, and then propagates back to a receiver antenna array [2]. The composition of the scene is then visualized by numerically generating an image that represents the positions and reflectivities of the objects in it. However, depending on the dielectric permittivity and permeability of the walls, the received signal is often corrupted with indirect multipath reflections from the front wall ringing as well as reflections off the internal walls, which result in ghost artifacts that clutter the reconstructed image. Suppressing such multipath reflections is an important topic that can significantly improve the quality of TWI and enhance the applicability of the technique.

The centrality of multipath suppression has resulted in the development of many practical solutions to the problem. Earlier works considered the problem of multipath elimination by assuming a perfect knowledge of the reflective geometry of the scene. For example, Setlur *et al.* [3, 4] have developed multi-path signal models to associate the multi-path ghosts to the true target locations, thereby improving the radar system performance by reducing false positives in the original SAR image. Chang [5] proposed a physics based approach to multi-path exploitation where the imaging kernel of the back-projection method is designed to focus on specific propagation paths of interest. Leigsnering *et al.* [6] combined target sparsity with multi-path modeling to achieve further improvements in the quality of TWI. Specifically, their approach incorporates the sources of multi-path reflections of interest into a sparsifying dictionary and solves a group sparse recovery problem to locate the targets from randomly subsampled, frequency stepped SAR data. The current trend in literature is to formulate TWI as a blind sparse-recovery problem, where scene parameters are not known. Mansour and Liu [7] proposed a multipath-elimination by sparse inversion (MESI) algorithm that removes the clutter by iteratively recovering the primary impulse responses of targets followed by estimation of corresponding convolution operators that result in multi-path reflections in the received data. More recently, Leigsnering *et al.* [8] have extended their earlier sparsity-based muti-path exploitation framework by allowing for uncertainties in wall-parameters that are solved via an alternating optimization scheme.

In this paper, we propose an online sparse imaging with blind deconvolution scheme that jointly estimates a sparse target scene and removes the multipath reflections induced by front wall ringing. We specifically address in section 2 a received signal model where multipath reflections of all targets are generated by a convolution kernel that may change between different receivers. This setup is particularly suitable for large standoff TWI. Our proposed online scheme can be perceived as a stochastic gradient approach for sparse image reconstruction. We present in section 3 the proposed algorithm which relies on a modification of the sparse randomized Kaczmarz method of [9] to jointly perform sparse recovery and kernel deconvolution. Finally, we demonstrate the performance of our algorithm in section 4 using a simple FDTD simulated TWI setup with relatively large standoff distance. The numerical results highlight the ability of our approach to correctly suppress the wall ringing effect and detect the true targets, even those that exhibit weak reflections.

## 2. FRONT WALL RINGING MODEL

We consider a radar setup with $N_s$ transmitting sources and $N_r$ receiving antennas. Let $s(t)$ be the time-domain waveform of the pulse that is transmitted by each source, and denote by $g_p(t, n_r, n_s)$ the primary impulse response of the scene, excluding multi-path reflections, viewed at receiver $n_r \in \{1, \dots N_r\}$ as a reflection of a pulse transmitted from source $n_s \in \{1, \dots N_s\}$. Also denote by $g_m(t, n_r, n_s)$ the impulse response of the multi-path reflections due to the front wall ringing. Using a standard time-domain representation of the received signal model, we express the received signal $r(t, n_r, n_s)$ as follows

$$r(t, n_r, n_s) = s(t) * (g_p(t, n_r, n_s) + g_m(t, n_r, n_s)), \quad (1)$$

where $*$ is the convolution operator.

Without loss of generality, suppose that there are $K$ target objects in the scene, each inducing a primary impulse response $g_k(t, n_r, n_s)$ indexed by $k \in \{1 \dots K\}$. The multiples' impulse response can then be modeled by the convolution of a delay kernel $d(t, n_r, n_s)$ with the primary impulse response $g_k(t, n_r, n_s)$ of each target object in the scene, such that,

$$\begin{aligned} g_p(t, n_r, n_s) &= \sum_{k=1}^{K} g_k(t, n_r, n_s), \\ g_m(t, n_r, n_s) &= d(t, n_r, n_s) * \left( \sum_{k=1}^{K} g_k(t, n_r, n_s) \right). \end{aligned} \quad (2)$$

Here we assume that, for a particular transmitter-receiver pair $(n_r, n_s)$, all primary target reflections experience the same delay convolution kernel $d(t, n_r, n_s)$ when generating the wall ringing. This assumption is suitable when there is a large standoff distance between the antennas and the front wall. The delay kernel can be regarded as a weighted Dirac delta train

$$d(t) = \sum_{p} w_p \delta(t - t_p),$$

where $t_p > 0$ is the time delay at which the multiple reaches the receiver from the $p$th multi-path source, $w_p$ is the attenuation weight of the $p$th path.

We extend the definition of the delay kernel $d(t, n_r, n_s)$ to that of an activation function that generates both the primary and multiple impulse responses by allowing $t_j \geq 0$. Consequently, the received signal model can be written as the superposition of the primary responses of all $K$ objects in the scene convolved with an activation function as follows

$$r(t, n_r, n_s) = s(t) * \sum_{k=1}^{K} d(t, n_r, n_s) * g_k(t, n_r, n_s), \quad (3)$$

where $d(t, n_r, n_s)$ is independent of $k$.

## 3. ONLINE MULTIPATH ELIMINATION

We follow a two stage stochastic gradient approach similar in spirit to [10]. Given a measurement $r(t, n_r, n_s)$, we first estimate the activation kernel $d(t, n_r, n_s)$. Then, we compute a stochastic gradient update of the image based on $r(t, n_r, n_s)$ and the estimated $d(t, n_r, n_s)$.

### 3.1. Multipath elimination as a nonlinear inverse problem

In a blind through the wall imaging scenario, we have no information about the wall parameters or the number of targets present in the scene. Our objective is to identify the true target locations and remove the ghost targets using only the received signals $r(t, n_r, n_s)$ and the source waveform $s(t)$.

Denote by $\mathbf{r}_{n_r,n_s} \in \mathbb{R}^{N_t}$ the received signal at transmitter and receiver locations $(n_r, n_s)$, where $N_t$ is the number of time samples recorded by a receiver for each transmission. Also denote by $\mathbf{d}_{n_r,n_s} \in \mathbb{R}^{N_t}$ the vectorized time-domain activation function. Let $\mathbf{S} : \mathbb{R}^{N_t} \to \mathbb{C}^{N_f}$ be the source waveform matched-filtering operator that maps $\mathbf{r}_{n_r,n_s}$ to its frequency domain matched-filtered response $\hat{\mathbf{r}}_{n_r,n_s} = \mathbf{S}\mathbf{r}_{n_r,n_s}$, where $N_f$ is the number of sampled frequency bins. We discretize the scene into an $N_x \times N_y \times N_z$ grid and construct the imaging operator $\mathbf{G}_{n_r,n_s} : \mathbb{C}^{N_f} \to \mathbb{C}^{N_x N_y N_z}$ that maps $\hat{\mathbf{r}}_{n_r,n_s}$ to the image $\mathbf{x}$, such that

$$\mathbf{G}_{n_r,n_s}(\omega, l) = e^{\mathrm{i}\omega(\|\phi(l)-\phi(n_r)\|_2 + \|\phi(l)-\phi(n_s)\|_2)/c}, \quad (4)$$

where $\omega$ is the frequency in radians, $l$ is a spatial index in $N_x \times N_y \times N_z$, $c$ is the speed of the wave in free space, and $\phi(\cdot) \in \mathbb{R}^3$ gives the spatial coordinate vector of scene index $l$, receiver $n_r$, and transmitter $n_s$. The received signal model in (3) can now be expressed as a function of the image $\mathbf{x}$ as $\mathbf{r}_{n_r,n_s} = \mathbf{d}_{n_r,n_s} * \mathbf{S}^H \mathbf{G}^H_{n_r,n_s} \mathbf{x}$.

Denote by $\mathbf{A}_j$ the $N_t \times N_x N_y N_z$ matrix $\mathbf{A}_j = \mathbf{S}^H \mathbf{G}_j^H$ where $j$ indexes transmitter-receiver pairs $(n_r, n_s) \in [N_r] \times [N_s]$. Also, let $\mathbf{r}_j = \mathbf{r}_{n_r,n_s}$ for the transmitter-receiver pair indexed by $j$. The combined imaging and multipath removal problem can now be formulated as the following nonlinear inverse problem

$$\min_{\mathbf{x}, \mathbf{d}_j \forall j} \frac{1}{2} \sum_j \|\mathbf{r}_j - \mathbf{d}_j * \mathbf{A}_j \mathbf{x}\|_2^2. \quad (5)$$

For known activation kernels $\mathbf{d}_j$, problem (5) becomes a large overdetermined least squares problem for which a multitude of solvers exist. We discuss below one particularly efficient solution using the Kaczmarz method.

### 3.2. The Kaczmarz method

The Kaczmarz method [11] is an algorithm for finding the solution $\mathbf{x}$ of large overdetermined systems of linear equations $\mathbf{A}\mathbf{x} = \mathbf{r}$, where $\mathbf{A} \in \mathbb{C}^{M \times N}$ has full column rank and $\mathbf{r} \in \mathbb{C}^M$. The algorithm sequentially cycles through the rows of $\mathbf{A}$, orthogonally projecting the solution estimate at iteration $j$ onto the solution space given by a row or block of rows $\mathbf{A}_j$, such that

$$\mathbf{x}_j = \mathbf{x}_{j-1} + \mathbf{A}_j^H \frac{\mathbf{r}_j - \langle \mathbf{A}_j, \mathbf{x}_{j-1} \rangle}{\|\mathbf{A}_j\|_2^2}. \quad (6)$$

Several works in the literature have shown that randomizing the row selection criteria improves the convergence performance of the Kaczmarz method [12]. It was also shown in [13] that the randomized Kaczmarz method reaches an error threshold dependent on the matrix $\mathbf{A}$ in the case when the measurements are noisy. More recently, the randomized Kaczmarz update rule was shown to be an instance of stochastic gradient descent [14].

In [9], a sparse randomized Kaczmarz (SRK) algorithm was proposed that projects the iterate $\mathbf{x}_{j-1}$ onto a subset of rows of $\mathbf{A}$ weighted by a diagonal matrix $\mathbf{W}_j$, i.e.

$$\mathbf{x}_j = \mathbf{x}_{j-1} + \mathbf{W}_j \mathbf{A}_j^H \frac{\mathbf{r}_j - \langle \mathbf{A}_j \mathbf{W}_j, \mathbf{x}_{j-1} \rangle}{\|\mathbf{A}_j \mathbf{W}_j\|_2^2}. \quad (7)$$

The weighting is based on identifying, in each iteration $j$, a support estimate $T_j$ for $\mathbf{x}$ corresponding to the largest $\hat{k}$ entries of the iterate $\mathbf{x}_j$, where $\hat{k}$ is some predetermined sparsity level. The weighting gradually scales down the entries of $\mathbf{A}_j$ that lie outside of $T_j$ by a weight equal to $1/\sqrt{j}$. As the number of iterations becomes large, the weight $\frac{1}{\sqrt{j}} \to 0$ and the algorithm begins to resemble the randomized Kaczmarz method applied to the reduced system $\mathbf{A}_T \mathbf{x}_T = \mathbf{r}$, where $\mathbf{A}_T$ is a subset of the columns of $\mathbf{A}$ at which the sequence of sets $T_j$ converges. It was demonstrated empirically in [9] that the SRK method is capable of finding sparse solutions to both over and under-determined linear systems, and enjoys faster convergence compared to the randomized Kaczmarz algorithm of [12]. The SRK update iteration can then be used to incrementally compute the image $\mathbf{x}$ by setting $\mathbf{r}_j = \mathbf{r}_{n_r,n_s}$ and $\mathbf{A}_j = \mathbf{A}_{n_r,n_s}$ using different transmitter-receiver pairs $(n_r, n_s)$ in every iteration $j$.

### 3.3. Sparse Kaczmarz with Multipath Deconvolution

Define the linear operator $\mathcal{H} : \mathbb{R}^{N_t \times N_t} \to \mathbb{R}^{N_t}$ that computes the non-circular convolution of two vectors $\mathbf{u}, \mathbf{v} \in \mathbb{R}^{N_t}$ by summing the anti-diagonal entries of their outer product matrix $\mathbf{u}\mathbf{v}^T$. Consequently, the adjoint $\mathcal{H}^T$ of $\mathcal{H}$ applied to a vector $\mathbf{v}$ repeats the entries of $\mathbf{v}$ along the anti-diagonal entries of an $N_t \times N_t$ matrix.

We cast the sparse deconvolution problem as the following non-convex constrained optimization problem

$$\begin{array}{ll} \min\limits_{\mathbf{x},\mathbf{d}_j \forall j} & \frac{1}{2}\sum\limits_j \|\mathbf{r}_j - \mathcal{H}\left((\mathbf{A}_j\mathbf{x})\mathbf{d}^T\right)\|_2^2 \\ \text{subject to} & \|\mathbf{x}\|_0 \leq p, \|\mathbf{d}\|_0 \leq q, \end{array} \tag{8}$$

where $j$ indexes transmitter-receiver pairs $(n_r, n_s) \in N_r \times N_s$, and $p$ and $q$ are predetermined bounds on the sparsities of $\mathbf{x}$ and $\mathbf{d}$, respectively. In what follows, denote by $\mathbf{x}^*$ the target sparse image of the scene.

Algorithm 1 presents an iterative two-stage heuristic for finding local solutions to (8) based on weighted gradient update for $\mathbf{d}_j$ and sparse Kaczmarz updates for $\mathbf{x}$. In the first stage, we fix $\mathbf{x} = \mathbf{x}_{j-1}$ and solve for $\mathbf{d}_j$ that minimizes

$$\mathbf{d}_j = \arg\min_{\mathbf{d}} \frac{1}{2}\|\mathbf{r}_j - \mathcal{H}\left((\mathbf{A}_j\mathbf{x}_{j-1})\mathbf{d}^T\right)\|_2^2 \text{ s.t. } \|\mathbf{d}\|_0 \leq q. \tag{9}$$

Problem (9) can be solved using iterative hard thresholding [15] for example. Here, we adopt a milder update rule where all components smaller than the top $q$ are weighted down by $1/\sqrt{l}$, where $l$ is the inner loop iteration number. In the second stage, we set $\mathbf{d} = \mathbf{d}_j$ and deconvolve it from the received signal to produce an estimate of the multipath suppressed signal $\hat{\mathbf{r}}_j$. We then solve for $\mathbf{x}_j$ that minimizes

$$\mathbf{x}_j = \arg\min_{\mathbf{x}} \frac{1}{2}\|\mathbf{W}_j(\mathbf{x} - \mathbf{x}_{j-1})\|_2^2 \text{ s.t. } \hat{\mathbf{r}}_j = \mathbf{A}_j\mathbf{x}. \tag{10}$$

The inputs to the algorithm are the measurements $\mathbf{r}_j$, the imaging operators $\mathbf{A}_j$, the activation function sparsity $q$, the image domain sparsity $p$, and step sizes $\eta$ and $\hat{\eta}$. The algorithm uses a sparse initial estimate of the image $\mathbf{x}_0 = \mathcal{T}_{\text{hard}}\left(\mathbf{A}_1^H\mathbf{r}_1; \tau\right)$ which we compute as a hard-thresholding of $\mathbf{A}_1^H\mathbf{r}_1$ using some large threshold $\tau$. The support function of a vector $\mathbf{x}$ that finds the index set of the largest $p$ entries in magnitude of $\mathbf{x}$ is denoted by $\text{supp}(\mathbf{x}|_p)$. The update rule in (10) is an oblique projection of $\mathbf{x}_{j-1}$ onto the hyperplane $\hat{\mathbf{r}}_j = \mathbf{A}_j\mathbf{x}$. This is in contrast with the RK and SRK updates which orthogonally project $\mathbf{x}_{j-1}$ onto $\hat{\mathbf{r}}_j = \mathbf{A}_j\mathbf{x}$ and $\hat{\mathbf{r}}_j = \mathbf{A}_j\mathbf{W}_j\mathbf{x}$, respectively. Notice that using the oblique projection, the entries of $\mathbf{x}_j$ on the complement $T^c$ of the support set $T$ are updated with the scaling $1/\sqrt{j}$. This may result in residual coefficients in $T^c$ that should be zero but are not suppressed, which leads to decreasing the angle $\theta_{\mathbf{W}\mathbf{A}_j}$ between $\mathbf{W}_j\mathbf{A}_j^H$ and $\mathbf{x}_{j-1} - \mathbf{x}^*$, compared to the angle $\theta_{\mathbf{A}_j}$ between $\mathbf{A}_j^H$ and $\mathbf{x}_{j-1} - \mathbf{x}^*$. Since the Kaczmarz update steps are essentially projections along some weighted $\mathbf{A}_j$, we want to maximize the angle between $\mathbf{x}_{j-1} - \mathbf{x}^*$ and the projection direction. Therefore, we compute proxies for the cosines of $\theta_{\mathbf{W}\mathbf{A}_j}$ and $\theta_{\mathbf{A}_j}$ and update $\mathbf{x}_j$ along the direction with the largest angle.

**Algorithm 1** Sparse Kaczmarz with Clutter Deconvolution

**Input** $\mathbf{r}_j$, $\mathbf{A}_j$, $p$, $q$, $\eta$, $\hat{\eta}$, `maxiter`
**Output** $\mathbf{x}$, $\mathbf{d}_j\ \forall j \in \{1, \dots N_rN_s\}$
**Initialize** $j = 0$, $\mathbf{d}_0 = [1, 0, \dots 0]^T$, $\mathbf{x}_0 = \mathcal{T}_{\text{hard}}\left(\mathbf{A}_1^H\mathbf{r}_1; \tau\right)$
**repeat**
  $j = j + 1$
  $\mathbf{y}_j = \mathbf{A}_j\mathbf{x}_{j-1}$
  $\mathbf{d}_j = \mathbf{d}_{j-1}$
  **for** $l = 1$ **to** `maxiter` **do**
    $T = \text{supp}(\mathbf{d}_j|_q)$
    $\mathbf{Q} = \mathbf{I}/\sqrt{l}$, $\mathbf{Q}_T = 1$
    $\mathbf{d}_j = \mathbf{Q}\left(\mathbf{d}_j + \eta\, \mathcal{H}^T\left(\mathbf{r}_j - \mathbf{d}_j * \mathbf{y}_j\right)\mathbf{y}_j\right)$
  **end for**
  $\hat{\mathbf{r}}_j = \mathbf{0}$
  **for** $l = 1$ **to** `maxiter` **do**
    $\hat{\mathbf{r}}_j = \hat{\mathbf{r}}_j + \hat{\eta}\, \mathcal{H}^T\left(\mathbf{r}_j - \mathbf{d}_j * \hat{\mathbf{r}}_j\right)\mathbf{d}_j$
  **end for**
  $T = \text{supp}(\mathbf{x}_j|_p)$
  $\mathbf{W} = 1/\sqrt{j}$, $\mathbf{W}_T = 1$
  **if** $\frac{\|\hat{\mathbf{r}}_j - \mathbf{A}_j\mathbf{W}\mathbf{x}_{j-1}\|_2}{\|\mathbf{A}_j\mathbf{W}\|_F} > \frac{\|\hat{\mathbf{r}}_j - \mathbf{A}_j\mathbf{x}_{j-1}\|_2}{\|\mathbf{A}_j\|_F}$ **then**
    $\mathbf{x}_j = \mathbf{x}_{j-1} + \frac{1}{\|\mathbf{A}_j\mathbf{W}\|_F^2}\mathbf{W}\mathbf{A}_j^H\left(\hat{\mathbf{r}}_j - \mathbf{A}_j\mathbf{x}_{j-1}\right)$
  **else**
    $\mathbf{x}_j = \mathbf{W}\left(\mathbf{x}_{j-1} + \frac{1}{\|\mathbf{A}_j\|_F^2}\mathbf{A}_j^H\left(\hat{\mathbf{r}}_j - \mathbf{A}_j\mathbf{x}_{j-1}\right)\right)$
  **end if**
**until** $j \geq N_rN_s$

## 4. EXPERIMENTAL RESULTS

We asess the performance of our algorithm for identifying true target locations inside a room using measurements from an antenna array located outside the room. We generate a simple scene using a two-dimensional FDTD simulator. The scene dimensions are 3m×3m with the antenna array centered at position $(0.3, 1.5)$ and a 1.5m standoff distance from the front wall of the room. Fig. 1a illustrates the locations of the antenna array relative to the room which contains 7 cylindrical targets. The walls are composed of two layers, with a thickness and relative permittivity of 3cm and $\epsilon_r = 10$ for the outer layer, and 1.2cm and $\epsilon_r = 5$ for the inner layer, respectively. The antenna array is composed of 21 receiving elements with a 3cm spacing and a single transmitting element placed at the center of the array. The transmitter emits a Gaussian pulse with a 13GHz bandwidth and a mode located at 6.5GHz. The algorithm input parameters are set to: $p = 0.02N_xN_y$, $q = 0.01N_t$, $\eta = 2/N_t$, and $\hat{\eta} = 1/\sqrt{N_t}$.

Fig. 1b–1f shows the results of imaging the scene from 1b measurements of the targets obtained without having a room wall, and 1c–1f measurements of the targets with the room walls. The true locations of the seven targets are outlined by the red circles. Fig. 1c shows the multipath artifacts that arise when we reconstruct the image using standard backprojection after time gating the initial reflection from outside the front wall. On the other hand, using sparse recovery without deconvolving the multipath kernel results in Fig. 1d, which shows only a slight reduction in the multipath artifacts. Next we use Algorithm 1 to deconvolve the multipath kernel and reconstruct the image. Figs. 1e and 1f illustrate the reconstructed images using Algorithm 1 from sequential and randomized antenna locations, respectively. Notice that randomizing the antenna locations improves the ability to suppress multipath reflections compared to imaging from sequential measurements. The detected convolution kernel is shown in Fig. 2.

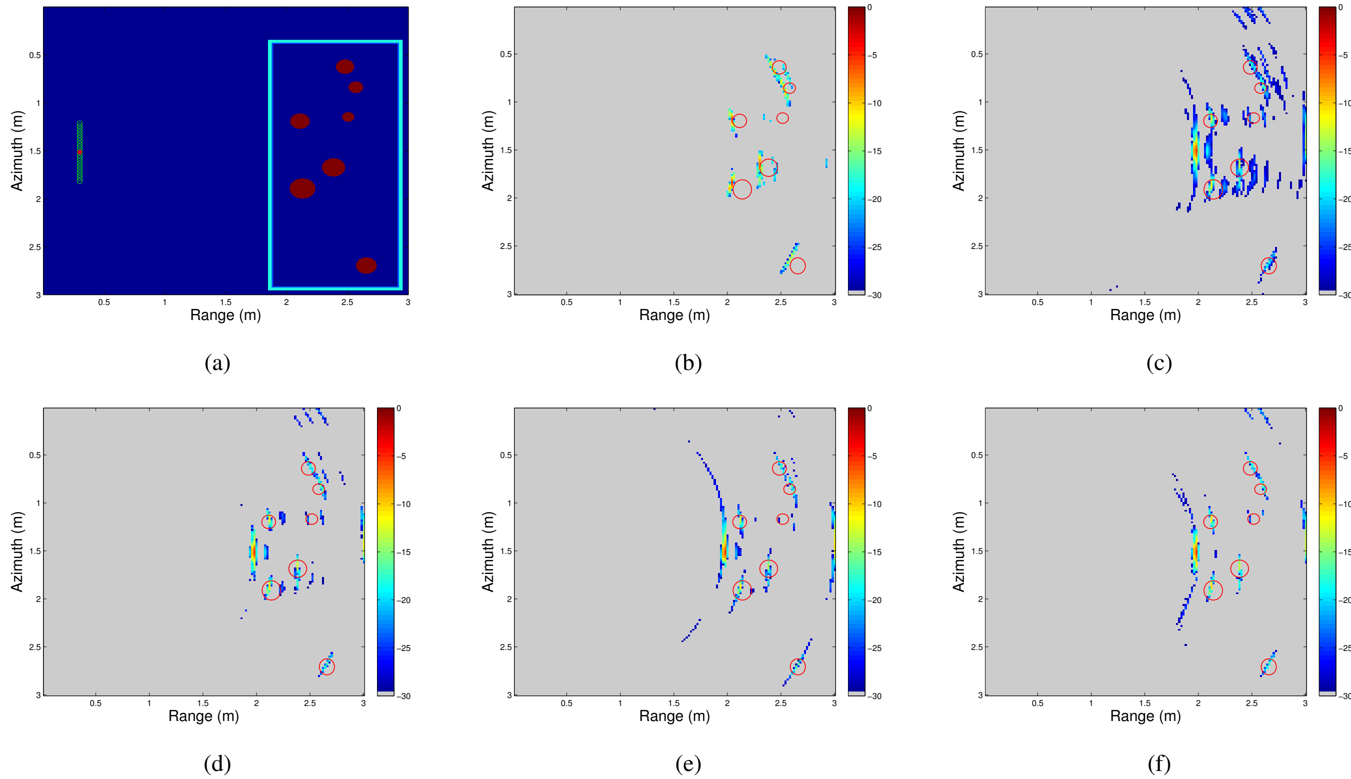


**Fig. 1**. (a) Schematic of the simulation layout where the color bar indicates the relative permittivity. (b)–(e) Imaging results in dB of the simulated scene with the targets outlined by red circles for (b) measurements without the room walls, and measurements with the room walls using (c) standard backprojection, and (d) sparse imaging using sparse Kaczmarz updates. (e)–(f) show the recovery using sparse Kaczmarz with clutter deconvolution where the measurements are (e) sequential and (f) randomized.

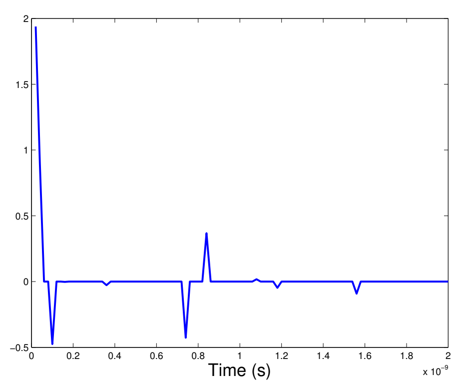


**Fig. 2**. Recovered multipath convolution kernel using Algorithm 1 from randomized antenna locations.

## 5. DISCUSSION AND CONCLUSION

We attribute the different imaging performance between randomized and sequential measurements to the high correlation between the sequential measurements that is overcome by randomization. In both cases, it can be seen that the multipath reflections due to the side walls remain visible in the image. This is due to the delay convolution multipath model that we use which specifically targets front wall ringing. Without knowledge of the side wall orientation and position as is assumed in [6, 8], it is not possible to compensate for the side wall multipath effect.

The sparse randomized Kaczmarz with clutter deconvolution algorithm attempts to solve a structured version of problem (5). The difficulty in joint online imaging and deconvolution is that a single measurement $\mathbf{r}_j$ does not admit a unique representation in $\mathbf{x}_j$ and $\mathbf{d}_j$. However, the stationarity of the scene allows us to find a common sparse image $\mathbf{x}$ that best matches the measurements while relegating the variability between measurements to the convolution operator $\mathbf{d}$. In this respect, we emphasize the importance of randomizing the order of measurements since randomization mitigates the correlations between subsequent measurements. Our online scheme is memory efficient especially in the case where the antennas are not located on a uniform grid. Moreover, our signal model defines a single convolution kernel that maps all targets to their multipath reflections for a particular receiver. This is in contrast to MESI [7] which relies on the availability of all measurements and models a distinct multipath kernel for each target common to all receivers.

## 6. REFERENCES


[1] M. G. Amin and F. Ahmad, "Through-the-wall radar imaging: Theory and applications," *Radar Signal Processing Section, E-Reference Signal Processing, Elsevier*, 2013.

[2] T. S. Ralston, G. L. Charvat, and J. E. Peabody, "Real-time through-wall imaging using an ultrawideband multiple-input multiple-output (MIMO) phased array radar system," in *IEEE International Symposium on Phased Array Systems and Technology (ARRAY)*, 2010, pp. 551–558.

[3] P. Setlur, M. Amin, and F. Ahmad, "Multipath model and exploitation in through-the-wall and urban radar sensing," *IEEE Transactions on Geoscience and Remote Sensing*, vol. 49, no. 10, pp. 4021–4034, 2011.

[4] P. Setlur, G. Alli, and L. Nuzzo, "Multipath exploitation in through-wall radar imaging via point spread functions," *IEEE Transactions on Image Processing*, vol. 22, 2013.

[5] P. C. Chang, *Physics-Based Inverse Processing and Multi-path Exploitation for Through-Wall Radar Imaging*, Ph.D. thesis, Ohio State University, 2011.

[6] M. Leigsnering, F. Ahmad, M. Amin, and A. Zoubir, "Multipath exploitation in through-the-wall radar imaging using sparse reconstruction," *IEEE Trans. Aerosp. Electron. Syst.*, vol. 50, no. 2, pp. 920–939, April 2014.

[7] H. Mansour and D. Liu, "Blind multi-path elimination by sparse inversion in through-the-wall-imaging," in *Proc. IEEE 5th Int. Workshop on Computational Advances in Multi-Sensor Adaptive Process. (CAMSAP)*, St. Martin, December 15-18, 2013, pp. 256–259.

[8] M. Leigsnering, F. Ahmad, M. G Amin, and A. M. Zoubir, "CS based specular multipath exploitation in TWRI under wall position uncertainties," in *Proc. 8th IEEE Sensor Array and Multichannel Signal Processing Workshop*, Coruña, Spain, June 22-25, 2014, pp. 481–484.

[9] H. Mansour and O. Yilmaz, "A sparse randomized Kaczmarz algorithm," in *IEEE Global Conference on Signal and Information Processing (GlobalSIP)*, Dec 2013, pp. 621–621.

[10] S. Harmeling, M. Hirsch, S. Sra, and B. Scholkopf, "Online blind deconvolution for astronomical imaging," in *IEEE International Conference on Computational Photography (ICCP)*, April 2009, pp. 1–7.

[11] S. Kaczmarz, "Angenäherte Auflösung von Systemen linearer Gleichungen.," *Bull. Int. Acad. Polon. Sci. A*, vol. 1937, pp. 355–357, 1937.

[12] T. Strohmer and R. Vershynin, "A randomized Kaczmarz algorithm with exponential convergence," *Journal of Fourier Analysis and Applications*, vol. 15, pp. 262 – 278, 2009.

[13] D. Needell, "Randomized Kaczmarz solver for noisy linear systems," *BIT Numerical Mathematics*, vol. 50, no. 2, pp. 395–403, 2010.

[14] D. Needell, N. Srebro, and R. Ward, "Stochastic gradient descent, weighted sampling, and the randomized Kaczmarz algorithm," *http://arxiv.org/abs/1310.5715*, 2014.

[15] T. Blumensath and M. E. Davies, "Iterative thresholding for sparse approximations," *Journal of Fourier Analysis and Applications*, vol. 14, no. 5-6, pp. 629–654, 2008.